32nd URSI GASS, Montreal, 19–26 August 2017

Occurrence characteristics of relativistic electron microbursts from SAMPEX observations

Emma Douma*(1), Craig J. Rodger(1), Lauren W. Blum(2), and Mark A. Clilverd(3)
(1) Department of Physics, University of Otago, Dunedin, New Zealand
(2) NASA Goddard Space Flight Center, Greenbelt MD, USA
(3) British Antarctic Survey (NERC), Cambridge, United Kingdom

Abstract

We study the occurrence of relativistic microbursts observed by the Solar Anomalous Magnetospheric Particle Explorer (SAMPEX) satellite. We identify 193,694 relativistic microbursts in the > 1.05 MeV electron fluxes occurring across the time period from 1996 to 2007. Our observations are normalized to provide the change in absolute occurrence rates with various parameters. We find that the L and MLT distribution of relativistic microbursts is consistent with the L and MLT distribution of whistler mode chorus amplitude. The peak relativistic microburst occurrence frequency moves to lower L as the geomagnetic activity increases, reaching a peak occurrence rate of one microburst every 10.4 s (on average) at $L = 4$ when $6.6 \leq \mathrm{Kp} \leq 8.7$. The L and MLT distribution of the relativistic microbursts exhibit a peak occurrence of one microburst every 8.6 (98.0) s during active (disturbed) conditions, with the peak located at $L = 5$ ($L = 5.5$) and 08 (08) MLT.

1 Introduction

Relativistic electron microbursts are intense short-duration (< 1 s) precipitation events of > 1 MeV electrons from the outer radiation belt into the atmosphere [1]. It has been suggested that relativistic microbursts occurring during a single storm could empty the entire relativistic electron population [2]. Thus, it is important to better understand the conditions under which relativistic microbursts occur, as well as the physical processes in space which drive this type of precipitation.

Many previous studies have been undertaken on relativistic microbursts using various satellites. However, the majority of relativistic microburst studies thus far have only considered relatively short time periods, ranging from a few case study storms [2] to a few months of data [5]. Studies using longer time periods have focused on particular storm types, for example [4] only considered High Speed Stream (HSS) driven storms. This is a deficiency we correct in the current study.

Relativistic microbursts are most often observed in the morning Magnetic Local Time (MLT) sector, between midnight and noon [3, 4, 5]. Relativistic microbursts primarily occur in the L = 3.5 - 6 region [4, 5] with the greatest frequency of occurrence at $L = 5$ [3]. Relativistic microburst occurrence rates tend to increase during geomagnetically active periods and correlate strongly with variations in both Dst and Kp [2, 3]. Relativistic microbursts occur primarily outside the plasmapause [3] and generally move to lower L during geomagnetic storms [2, 4, 5].

It has been suggested for some time that relativistic microbursts are driven by pitch angle scattering of radiation belt electrons interacting with whistler mode chorus waves. However, at this stage there has been little direct experimental evidence to demonstrate this. Many studies in the current literature have concluded that their observations are consistent with chorus waves as the driver of relativistic microbursts. These arguments are based on an overlap, in both L and MLT space, of the active chorus regions with the microburst occurrence regions [3, 5], an approach we also use.

Recently a study was published by [6] focused upon anomalous cyclotron resonance between relativistic electrons (> 1 MeV) and electromagnetic ion cyclotron (EMIC) triggered emissions. These authors reported that this resonance is effective, resulting in the efficient precipitation of relativistic electrons (as microbursts) through nonlinear trapping by EMIC triggered emissions. This comparatively new theoretical work indicates there is uncertainty as to the dominant scattering process which leads to relativistic microbursts, suggesting that the occurrence of these precipitation events may need to be re-examined.

In this paper we use the method in [3] to produce a very large database of SAMPEX relativistic microburst detections across a long time period, and over a broad range of geomagnetic conditions. We reliably correct for the sampling bias in the satellite observations, establishing for the first time the absolute relativistic microburst occurrence rates. We examine the L and MLT distribution of relativistic microbursts and compare the L and MLT distribution of relativistic microbursts to those of whistler mode chorus and EMIC waves, provided in the literature.

2 Experimental Dataset

The Solar Anomalous Magnetospheric Particle Explorer (SAMPEX) satellite was in a low altitude orbit (520 -

670 km) [7]. SAMPEX carried the Heavy Ion Large Telescope (HILT) instrument, which produced high sensitivity and high time resolution >1.05 MeV electron and >5 MeV proton flux measurements [8]. In the current study we use row 4 of the solid state detector array which has a temporal resolution of 100 ms. All available HILT data at the SAMPEX Data Centre from 8 August 1996 through to the end of the dataset on 3 November 2012 are included in our initial analysis. The HILT instrument responds to both electron and protons, thus, as an initial processing step we remove all data coinciding with solar proton events and periods when SAMPEX was inside the South Atlantic Magnetic Anomaly (SAMA), where inner belt protons will reach SAMPEX-altitudes.

3 Event Selection

We apply the microburst detection algorithm [3] to all the SAMPEX/HILT data from 23 August 1996 through to 3 November 2012 (after the removal of SPEs, SAMA regions, and times of spin mode). Unfortunately, the satellite was continuously in spin mode from late 2007 until re-entry, limiting us to the period from 23 August 1996 through to 11 August 2007. The detection algorithm is as follows:

$$\frac{N_{100} - A_{500}}{\sqrt{1 + A_{500}}} > 10. \quad (1)$$

where N_{100} is the number of counts in 100 ms and A_{500} is the centered running average of N_{100} over five 100 ms intervals (i.e., over 500 ms). It should be noted that the algorithm does not perform well at either low radiation belt fluxes, or during strong pitch angle diffusion [3], thus we will not consider relativistic microbursts occurring during quiet geomagnetic conditions.

Figure 1 is an example of the microbursts detected by the algorithm on 19 August 1999 from 14:05:30 to 14:06:30 UT, where each red cross (18 in total) is a trigger in the algorithm identified as a relativistic microburst. We detect 193,694 relativistic electron microbursts between 23 August 1996 and 11 August 2007, after which SAMPEX was in spin mode. In the following sections we will discuss the absolute occurrence rates of relativistic microbursts. We normalize the L and MLT distribution of relativistic microbursts by the number of satellite samples in each L/MLT bin.

4 Connection to Geomagnetic Activity

The L distribution of relativistic microbursts is highly dependent on the level of geomagnetic activity. This variation is presented in Figure 2 with five geomagnetic activity levels, all corrected for the satellite sampling bias. During quiet geomagnetic conditions, Kp $\leq$ 3 (the black bars in Figure 2), relativistic microbursts are very infrequent at all L values, with a peak occurrence of only 0.004 microbursts s^{-1} at L = 5.5. During disturbed geomagnetic conditions, 3 < Kp < 4.6 (the blue bars), relativistic microbursts become

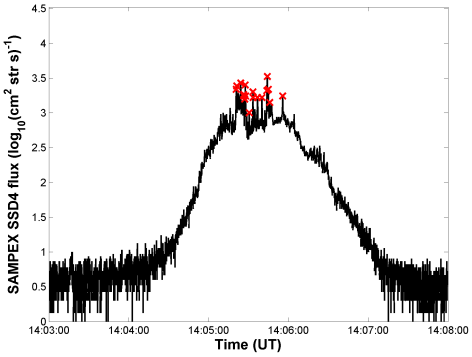

Figure 1. The SAMPEX >1.05 MeV HILT electron flux on 19 August 1999, with each red cross indicating a trigger from the microburst detection algorithm [3].

more frequent over the L values from 3 to 8 (note there is little microburst activity outside these L values), with a peak occurrence of 0.033 microbursts s^{-1} at L = 5. During moderate conditions, 4.6 $\leq$ Kp $\leq$ 6.4 (the green bars), relativistic microbursts have a peak occurrence of 0.068 microbursts s^{-1} at L = 5. The relativistic microbursts become most frequent for severe geomagnetic conditions, 6.6 $\leq$ Kp $\leq$ 8.7 (the red bars), with a peak occurrence of 0.096 microbursts s^{-1} at L = 4. This peak relativistic microburst occurrence rate of 0.096 microbursts s^{-1} equates to an average of 1 microburst occurring every 10.4 s. Our dataset does not contain any extreme geomagnetic conditions with Kp > 8.7. Thus, we observe that the microbursts become more frequent and the region of peak occurrence moves to lower L as the geomagnetic activity level increases.

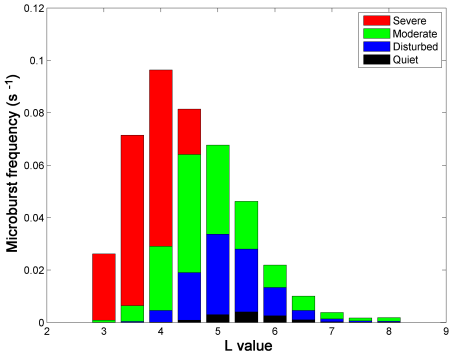

Figure 2. (a.) The L distribution of the relativistic microburst frequency for various geomagnetic activity levels. The black bars indicate quiet conditions (Kp $\leq$ 3), the blue bars indicate disturbed conditions (3 < Kp < 4.6), the green bars indicate moderate storms (4.6 $\leq$ Kp $\leq$ 6.4) while the red bars indicate severe storms (6.6 $\leq$ Kp $\leq$ 8.7).

5 Comparison with Chorus and EMIC occurrence characteristics

As discussed above it is often thought that whistler mode chorus waves are driving the pitch angle scattering which

lead to relativistic microbursts. However, recently there has been evidence published that EMIC waves could also produce relativistic microbursts. As a step towards answering which of the two waves are the dominant cause of relativistic microbursts we compare the L and MLT distribution of the relativistic microbursts with those published in the literature for chorus and EMIC waves. Figure 3 presents the L and MLT distribution of the relativistic microbursts at two different levels of geomagnetic activity as measured by AE*. Here we use the same definition of AE* as used by [9], where AE* is the mean of AE over the previous one hour. The L and MLT distributions of the relativistic microbursts presented in Figure 3 have a resolution of 0.5 L and 1 hour MLT. The colorbar describes the absolute frequency at which the relativistic microbursts occur on a log scale.

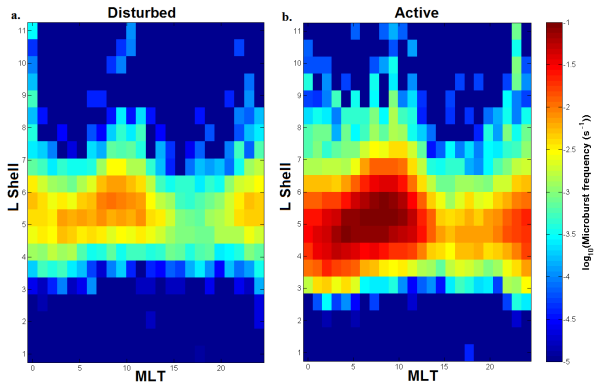

Figure 3. The L and MLT distribution of the relativistic microburst frequency during two levels of geomagnetic activity as measured by AE*. (a.) Disturbed conditions, defined as 100 < AE* $\leq$ 300 nT, and (b.) active conditions, defined as AE* > 300 nT.

5.1 Whistler mode chorus comparison

Relativistic microburst distributions are presented in Figure 3a for disturbed conditions and Figure 3b for active conditions. During both disturbed, 100 < AE* $\leq$ 300 nT, and active, AE* > 300 nT, geomagnetic conditions, the peak occurrence in the L and MLT distribution of relativistic microbursts is $\approx$0.01 microbursts s^{-1} at L = 5.5 and from 7 - 10 MLT (disturbed conditions) and $\approx$0.1 microbursts s^{-1} at L = 5 and from 6 - 10 MLT (active conditions). Furthermore, relativistic microbursts are frequent over a much larger continuous MLT range than previously reported, beginning prior to midnight and continuing through until noon i.e., from 21 MLT to 13 MLT. From both panels of Figure 3 it is clear that relativistic microbursts are mostly contained between L = 3 - 8.

To the best of our knowledge the L-MLT distribution of whistler mode chorus wave occurrence has not as yet been analyzed for different levels of geomagnetic activity. Thus we will compare the relativistic microburst occurrence rates with the results of previous studies examining whistler mode chorus wave amplitudes. The equatorial whistler mode root mean square chorus wave amplitude distribution for active and disturbed conditions reported by [9], has significant chorus activity at much lower L during disturbed and active geomagnetic conditions than that observed during quiet conditions. Further, stronger chorus wave amplitude is observed from MLT midnight through to noon (i.e., from 0 - 12 MLT) for disturbed conditions. During active conditions there is even stronger chorus wave amplitude observed prior to MLT midnight and through to post-noon (i.e., from 22 - 13 MLT). This strongly coincides with the relativistic microburst distributions we present in Figure 3. Therefore we conclude that the majority of relativistic microburst activity is consistent with a whistler mode chorus wave driver, in agreement with the previous speculation in the literature described above.

5.2 EMIC wave comparison

We find the L and MLT distributions of the relativistic microbursts are indistinguishable when the geomagnetic activity is defined by either AE or AE* so we will compare to EMIC wave distributions using either of the geomagnetic activity indices.

Overall EMIC waves are most often observed in the dayside outer magnetosphere. During moderate geomagnetic conditions (100 < AE < 300 nT) the peak occurrence of EMIC waves is at 8 - 17 MLT at $L \geq 4$ [10]. While during active conditions (AE > 300 nT) the peak occurrence of EMIC waves is in the afternoon MLT sector (12 - 18 MLT) from L = 4 - 6 with an occurrence rate of $\approx$25% [10]. More recently EMIC waves have also been observed in the dusk MLT sector (from 18 - 24 MLT) with occurrence rates increasing with geomagnetic activity [10]. That study found the average occurrence rate of EMIC waves in this MLT sector reach $\approx$15% over L = 4 - 6 during active geomagnetic conditions [10]. Comparing this to the L and MLT distribution of relativistic microbursts we note some similarities in the distributions. The EMIC activity observed during both moderate and active geomagnetic conditions from 8 - 17 MLT is coincident in L with the relativistic microburst activity along with the EMIC activity observed in the dusk sector, from 18 - 24 MLT. However, the frequent relativistic microburst activity from 24 - 8 MLT does not coincide with that seen in the patterns of EMIC activity. Therefore, only some of the relativistic microburst activity could be consistent with an EMIC wave driver.

6 Summary and Conclusions

We identify 193,694 relativistic microbursts in the >1.05 MeV electron fluxes occurring across the time period from 1996 to 2007. We find that relativistic microbursts are largely confined to the outer radiation belt, from L = 3 - 8 and occur primarily on the morning side, between 21 and 13 MLT. Relativistic microbursts become more frequent as the geomagnetic activity level increases, as measured by either Kp or AE*. The peak occurrence frequency of the

relativistic microbursts moves inward (to lower L) as the geomagnetic activity increases, to reach a peak occurrence rate of one microburst every 10.4 s at $L = 4$ for $6.6 \leq \text{Kp} \leq 8.7$.

During disturbed and active geomagnetic conditions, as measured by AE*, the L and MLT distribution of the relativistic microbursts have a peak occurrence of one microburst every 8.6 (98.0) s during active (disturbed) conditions at $L = 5$ ($L = 5.5$) and 08 (08) MLT. Whistler mode chorus waves have large amplitudes in the MLT region from 22 - 13 MLT coincident in L with the relativistic microburst activity. EMIC wave occurrence is most frequent from 8 - 17 MLT during both moderate and active conditions and from 18 - 24 MLT during active conditions, indicating some coincidence in L with the relativistic microburst activity. There are two regions of overlap from 8 - 13 MLT and from 22 - 24 MLT where the relativistic microbursts are consistent with scattering by either whistler mode chorus waves or EMIC waves. As relativistic microbursts are far more frequent in the 22 - 13 MLT region than other MLT regions our observations favor whistler mode chorus wave activity as the primary driver of relativistic microbursts during geomagnetically active periods.

Finally, we caution that correlation does not imply causation, and care must be taken in conclusions drawn from comparisons of the overall L and MLT distributions. Our study provides more suggestive evidence towards the potential linkages between these waves and the relativistic electron microbursts, as has been suggested by theory.

7 Acknowledgements

The authors would like to thank the many individuals involved in the operation of SAMPEX over 20 years. For the GOES data we acknowledge the Space Weather Prediction Center, Boulder, CO, National Oceanic and Atmospheric Administration (NOAA), US Dept. of Commerce. ED was supported by the University of Otago via a Fanny Evans PhD scholarship for women. LB was supported by the NSF AGS Postdoctoral Research Fellowship award #1524755. Data availability is described at the following websites: http://www.srl.caltech.edu/sampex/DataCenter/index.html (SAMPEX), wdc.kugi.kyoto-u.ac.jp (AE, Kp), ftp://spdf.gsfc.nasa.gov/pub/data/omni/high_res_omni/ (GOES protons).

References

[1] Blake, J. B., M. D. Looper, D. N. Baker, R. Nakamura, B. Klecker, and D. Hovestadt, "New high temporal and spatial resolution measurements by SAMPEX of the precipitation of relativistic electrons," *Advances in Space Research*, **18**, 8, December 1996, pp. 171–186, doi: 10.1016/0273-1177(95)00969-8.

[2] Lorentzen, K. R., M. D. Looper, and J. B. Blake, "Relativistic electron microbursts during the GEM storms," *Geophysical Research Letters*, **28**, 13, July 2001, pp. 2573–25768, doi: 10.1029/2001GL012926.

[3] O'Brien, T. P., K. R. Lorentzen, I. R. Mann, N. P. Meredith, J. B. Blake, J. F. Fennell, M. D. Looper, D. K. Milling, and R. R. Anderson, "Energization of relativistic electrons in the presence of ULF wave power and MeV microbursts: Evidence for dual ULF and VLF acceleration," *Journal of Geophysical Research: Space Physics*, **108**, A8, August 2003, A81329, doi: 10.1029/2002JA009784.

[4] Blum, L., X. Li, and M. Denton, "Rapid MeV electron precipitation as observed by SAMPEX/HILT during high-speed stream-driven storms," *Journal of Geophysical Research: Space Physics*, **120**, 5, May 2015, pp. 3783–3794, doi: 10.1002/2014JA020633.

[5] Nakamura, R., M. Isowa, Y. Kamide, D. N. Baker, J. B. Blake, and M. Looper, "SAMPEX observations of precipitation bursts in the outer radiation belt," *Journal of Geophysical Research: Space Physics*, **105**, A7, July 2000, pp. 15875–15885, doi: 10.1029/2000JA900018.

[6] Omura, Y., and Q. Zhao, "Relativistic electron microbursts due to nonlinear pitch angle scattering by EMIC triggered emissions," *Journal of Geophysical Research: Space Physics*, **118**, 8, August 2013, pp. 5008–5020, doi: 10.1002/jgra.50477.

[7] Baker, D. N., G. M. Mason, O. Figueroa, G. Colon, J. G. Watzin, and R. M. Aleman, "An Overview of the Solar, Anomalous, and Magnetospheric Particle Explorer (SAMPEX) Mission," *IEEE Transactions on Geoscience and Remote Sensing*, **31**, 3, May 1993, pp. 531–541, doi: 10.1109/36.225519.

[8] Klecker, B., D. Hovestadt, M. Scholer, H. Arbinger, M. Ertl, H. Kastle, E. Kunneth, P. Laeverenz, E. Seidenschwang, J. B. Blake, N. Katz, and D. Mabry, "HILT: A Heavy Ion Large Area Proportional Counter Telescope for Solar and Anomalous Cosmic Rays," *IEEE Transactions on Geoscience and Remote Sensing*, **31**, 3, May 1993, pp. 542–548, doi: 10.1109/36.225520.

[9] Li, W., R. M. Thorne, V. Angelopoulos, J. Bortnik, C. M. Cully, B. Ni, O. LeContel, A. Roux, U. Auster, and W. Magnes, "Global distribution of whistler-mode chorus waves observed on the THEMIS spacecraft," *Geophysical Research Letters*, **36**, 9, May 2009, L09104, doi: 10.1029/2009GL037595.

[10] Saikin, A. A., J.-C. Zhang, C. W. Smith, H. E. Spence, R. B. Torbert, and C. A. Kletzing, "The dependence on geomagnetic conditions and solar wind dynamic pressure of the spatial distributions of EMIC waves observed by the Van Allen Probes," *Journal of Geophysical Research: Space Physics*, **121**, 5, May 2016, pp. 4362–4377, doi: 10.1002/2016JA022523.